# cmgh

ORIGINAL RESEARCH

Vasoactive Intestinal Polypeptide Plays a Key Role in the Microbial–Neuroimmune Control of Intestinal Motility

Xiaopeng Bai,[1,2] Giada De Palma,[1] Elisa Boschetti,[3] Yuichiro Nishiharo,[1] Jun Lu,[1] Chiko Shimbori,[1] Anna Costanzini,[4] Zarwa Saqib,[1] Narjis Kraimi,[1] Sacha Sidani,[1] Siegfried Hapfelmeier,[5] Andrew J. Macpherson,[6] Elena F. Verdu,[1] Roberto De Giorgio,[7] Stephen M. Collins,[1] and Premysl Bercik[1]

[1]Farncombe Family Digestive Health Research Institute, Department of Medicine, McMaster University, Hamilton, Ontario, Canada; [2]Department of Medicine and Bioregulatory Science, Graduate School of Medical Sciences, Kyushu University, Fukuoka, Japan; [3]Department of Biomedical and NeuroMotor Sciences, University of Bologna, Bologna, Italy; [4]IRCCS Azienda Ospedaliero-Universitaria di Bologna, Bologna, Italy; [5]Institute for Infectious Diseases, University of Bern, Bern, Switzerland; [6]Department of Biomedical Research, University Hospital of Bern, Bern, Switzerland; and [7]Department of Translational Medicine, University of Ferrara, Ferrara, Italy
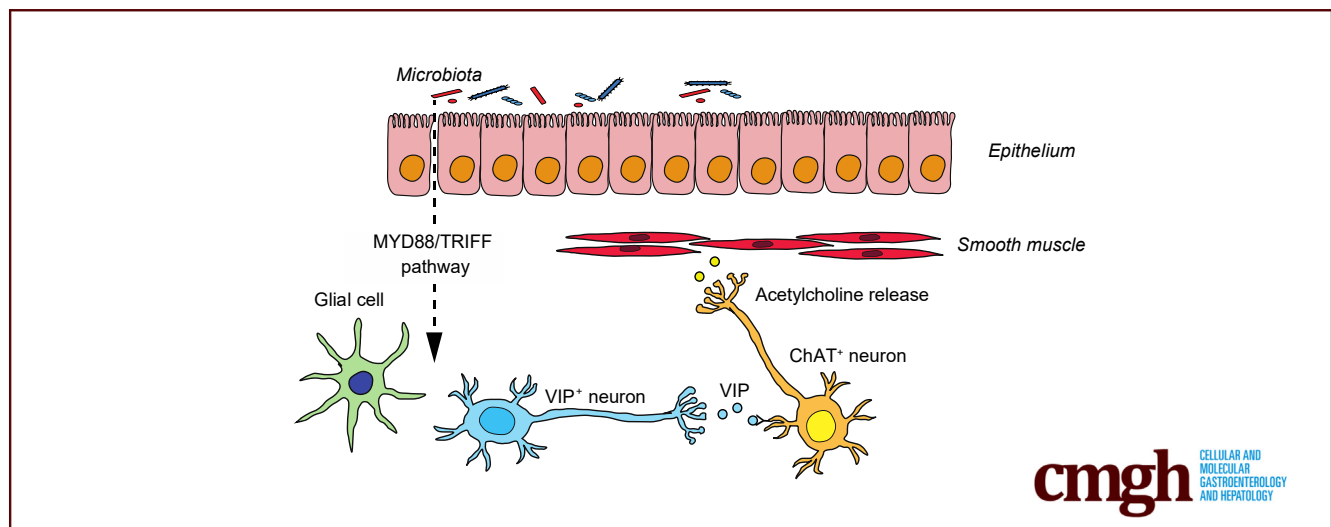
SUMMARY

We have identified a novel neuroimmune mechanism by which gut microbiota regulates intestinal motility that can lead to development of new treatments, including microbial therapeutics, targeting small intestinal VIP to treat chronic constipation and diarrhea.

BACKGROUND & AIMS: Although chronic diarrhea and constipation are common, the treatment is symptomatic because their pathophysiology is poorly understood. Accumulating evidence suggests that the microbiota modulates gut function, but the underlying mechanisms are unknown. We therefore investigated the pathways by which microbiota modulates gastrointestinal motility in different sections of the alimentary tract.

METHODS: Gastric emptying, intestinal transit, muscle contractility, acetylcholine release, gene expression, and vasoactive intestinal polypeptide (VIP) immunoreactivity were assessed in wild-type and $Myd88^{-/-}Trif^{-/-}$ mice in germ-free, gnotobiotic, and specific pathogen-free conditions. Effects of transient colonization and antimicrobials as well as immune cell blockade were investigated. VIP levels were assessed in human full-thickness biopsies by Western blot.

RESULTS: Germ-free mice had similar gastric emptying but slower intestinal transit compared with specific pathogen-free mice or mice monocolonized with *Lactobacillus rhamnosus* or *Escherichia coli,* the latter having stronger effects. Although muscle contractility was unaffected, its neural control was modulated by microbiota by up-regulating jejunal VIP, which co-localized with and controlled cholinergic nerve function. This process was responsive to changes in the microbial composition and load and mediated through toll-like receptor signaling, with enteric glia cells playing a key role. Jejunal VIP was lower in patients with chronic intestinal pseudo-obstruction compared with control subjects.

CONCLUSIONS: Microbial control of gastrointestinal motility is both region- and bacteria-specific; it reacts to environmental changes and is mediated by innate immunity-neural system

interactions. By regulating cholinergic nerves, small intestinal VIP plays a key role in this process, thus providing a new therapeutic target for patients with motility disorders. *(Cell Mol Gastroenterol Hepatol 2024;17:383–398; https://doi.org/10.1016/j.jcmgh.2023.11.012)*

See editorial on page 503.

Although functional diarrhea and constipation are very common, their treatment is symptomatic, because the pathophysiology is not well-understood.[1] This is in part due to our limited understanding of basic mechanisms governing gastrointestinal motility, including complex neuro-immune networks and microbial-host interactions.[2]

The role of microbiome in determining gut function has emerged during the last decades. It is now well-established that the microbiome shapes the mucosal immune system, regulates intestinal barrier, and affects visceral sensitivity and gastrointestinal motility.[3–5] Early studies demonstrated that germ-free rats have slower gastrointestinal transit compared with conventional rats.[6] Developmental studies then showed that during gestation bowel movements are weak but begin to normalize after birth,[7] accompanying microbial colonization and consequent maturation of the enteric nervous system. Gut microbiota affects the enteric nervous system and colonic motility by signaling through toll-like receptors (TLRs),[8,9] which are expressed by neurons and glial cells[10] as well as by maturation of colonic serotonin-containing cells and neural networks.[11,12]

Although the accumulated data suggest that microbial-neuro-immune interactions play a key role in gastrointestinal motility, the precise mechanisms are incompletely understood. Most previous work focused on the colon as the site of the highest bacterial biomass, whereas the small intestine with the highest density of immune cells in the digestive tract[13] has received relatively little attention.[14] Furthermore, microbial-neuro-immune mechanisms controlling motility likely differ between different sections of the digestive tract, reflecting different functions in sequential food processing, digestion, storage, and waste elimination.

Here we show that small intestinal motility, but not gastric emptying or colonic motility, is regulated by the microbiome through modulation of vasoactive intestinal polypeptide (VIP), which controls cholinergic nerve function. We demonstrate that this process is dynamic, dependent on TLR signaling, and likely mediated by enteric glial cells.

Results
Gut Microbiota Modulates Intestinal Transit but not Gastric Emptying

There was no difference in gastric emptying between specific pathogen-free (SPF) mice, germ-free mice, and mice monocolonized with non-pathogenic *Escherichia coli JM83* or *Lactobacillus rhamnosus X-32.2* (Figure 1*A*). However, intestinal transit was slower in germ-free mice, with most metallic beads found in the small intestine, compared with SPF mice or mice monocolonized with *E coli* or *L rhamnosus,* in which the beads were mainly localized in the cecum or colon (Figure 1*B*). Even though both groups of monocolonized mice showed faster intestinal transit than germ-free mice, it was more pronounced in *E coli*-monocolonized mice (Figure 1*B*), suggesting a differential modulation of gut function by specific bacterial strains.

Gut Microbiota Regulates Intestinal Contractility Through Cholinergic Nerves

To investigate underlying mechanisms, we studied jejunal and colonic tissue contractility in vitro. Equivalent KCl- or carbachol-stimulated muscle contractility in all groups indicated that myogenic function was unaffected by the gut microbiota (Figure 1*C* and *D*). To assess neural regulation, we used electric field stimulation (EFS)[15] in the presence or absence of tetrodotoxin or atropine. In SPF mice, EFS induced both jejunal and colonic contractility; this was preceded by strong relaxation in the colon and minor relaxation in the jejunum (Figure 1*E* and *F*). Tetrodotoxin blocked EFS-induced responses, confirming a neurogenic origin. Atropine administration decreased contractions in both the jejunum and colon and magnified the initial relaxation in the jejunum (Figure 1*E* and *F*), suggesting it is under cholinergic control.

The initial EFS-induced jejunal relaxation was much stronger in germ-free compared with SPF mice or mice colonized with *E coli*, whereas these microbiotas promoted EFS-stimulated contraction in the colon (Figure 1*G* and *H*), indicating that cholinergic nerves are regulated by the microbiota in a region-specific manner. Unlike *E coli*-monocolonized animals, responses in *L rhamnosus*-monocolonized mice were not different from those of germ-free mice (Figure 1*G* and *H*), indicating that specific bacterial species exert different effects on the host. EFS-induced [3H]-acetylcholine release[16] in the jejunum was lower in germ-free mice compared with SPF and *E coli*-monocolonized mice but similar to *L rhamnosus*-monocolonized mice (Figure 1*I*). We observed a similar pattern in the colon, but differences with selectively colonized mice did not reach statistical significance. Altogether, these data suggest that the presence of specific gut microbiota distinctly affect functional responses driven by the cholinergic system in the small intestine and the colon.
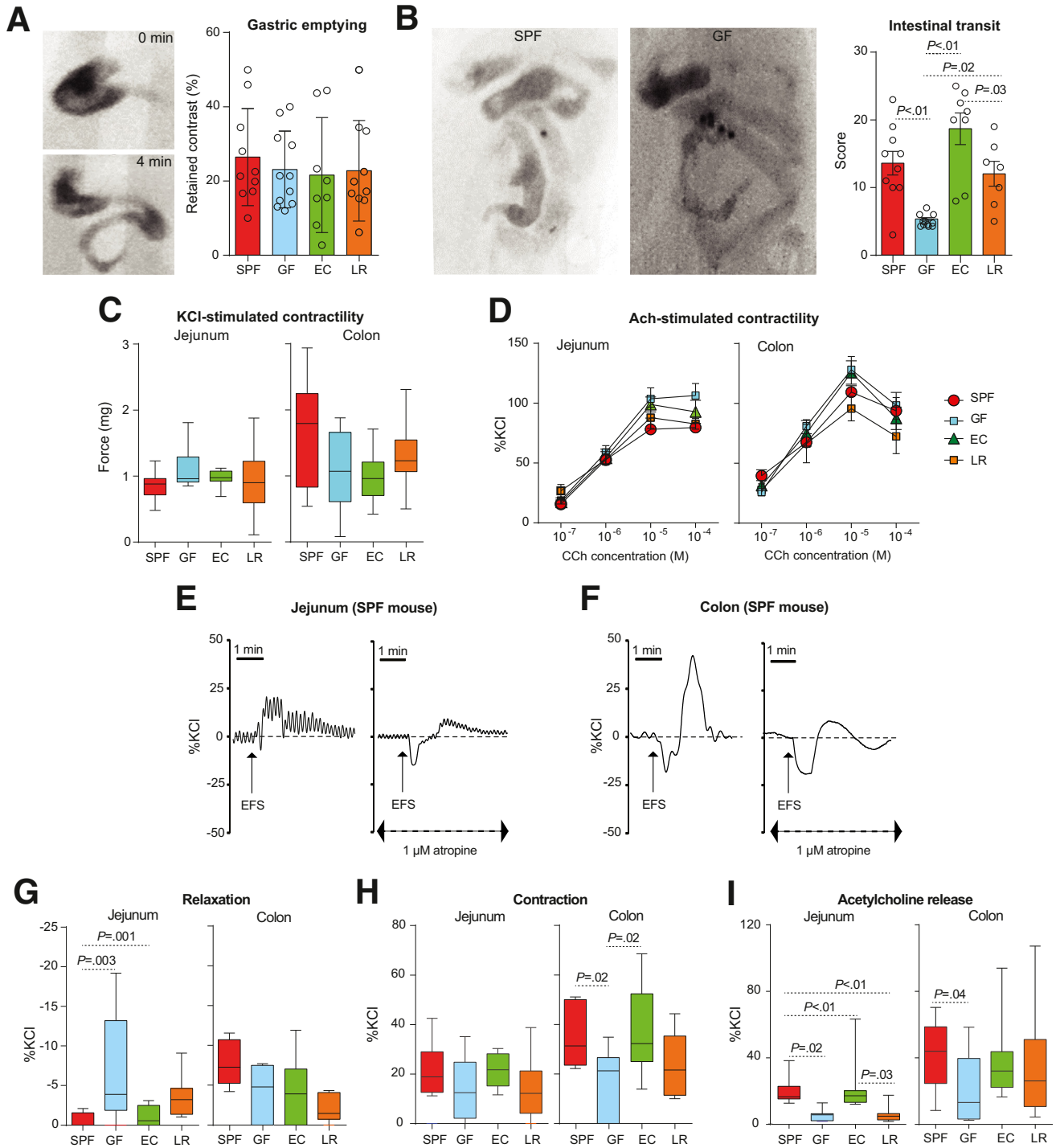
Most current article

Figure 1. Gastrointestinal motility in germ-free and colonized mice. (*A*) Representative photographs of mouse stomach (*left*) immediately after barium gavage and 3 minutes later. Gastric emptying results (*right*) in conventional (SPF, n = 10), germ-free (GF, n = 11), *E coli*-monocolonized (EC, n = 8), and *L rhamnosus*-monocolonized (LR, n = 8) mice. (*B*) Representative photographs (*left*) show only 1 bead in the ileum of SPF mouse and 5 beads in jejunum of GF mouse. Intestinal transit scores (*right*) in GF (n = 11), SPF (n = 10), EC (n = 8), and LR (n = 8) mice. (*C* and *D*) KCl- and CCh-induced contractility of tissues from SPF (n = 10), GF (n = 11), EC (n = 8), and LR (n = 8) mice. In *D*, force is expressed as a ratio to KCl-induced contraction in the same tissue. (*E* and *F*) Representative recordings of EFS-induced responses in tissues from SPF mouse, with and without presence of atropine. (*G* and *H*) EFS-induced relaxation and contraction of tissues from SPF (n = 10), GF (n = 11), EC (n = 8), and LR (n = 8) mice. (*I*) EFS-induced acetylcholine released from tissues of SPF (n = 13), GF (n = 10), EC (n = 12), and LR (n = 14) mice, expressed as a ratio to KCl-released acetylcholine in the same tissue.

Gut Microbiota Regulates VIP Control of Cholinergic Nerves

To identify putative mediators, we analyzed whole tissue gene expression in the jejunum and colon using a custom-designed Nanostring Codeset, which included genes related to regulation of muscle contractility such as choline acetyltransferase (*ChAT*), substance P (*Sp*), *Vip*, and nitric oxide synthase (*Nos*) (Figure 2*A* and *B*). Although there were no significant differences in *ChAT*, *Sp*, or *Nos* gene expression, *Vip* expression was lower in germ-free compared with SPF mice (Figure 3*A* and *B*). To verify the role of VIP in contractility, we pretreated intestinal tissues from SPF mice by combining VIP receptor 1 and 2 antagonists and then stimulated them with EFS. Pretreated jejunal tissues displayed increased relaxation and decreased contraction, whereas no significant effect was observed in the colon (Figure 3*C*), confirming that VIP regulates the activity of small intestinal cholinergic neurons as suggested by a previous study.[17] To explore in vivo effects of VIP, we administered a VIP analogue or saline to SPF mice using osmotic pumps. Mice that received the VIP analogue had faster intestinal transit (Figure 3*D*), further supporting the stimulatory role of VIP in intestinal motility.

To validate the expression of VIP and ChAT in the myenteric plexus, we performed immunofluorescence staining with anti-VIP, anti-ChAT, and anti-Hu antibodies. VIP-immunoreactive neurons and ChAT-immunoreactive neurons co-localized in the myenteric plexus of the jejunum of SPF mice (Figure 3*E*). Whereas the ChAT immunoreactivity levels were similar between SPF and germ-free mice (Figure 3*F*), in agreement with our gene expression data, VIP levels differed between germ-free, SPF, and *E coli*-monocolonized mice (Figure 3*G*), mirroring the intestinal transit results.

Although VIP gene expression in full-thickness colonic tissues was higher in SPF mice compared with germ-free mice (Figure 2*B*), VIP immunoreactivity in colonic myenteric plexus was similar between germ-free and SPF mice (Figure 3*H*), likely reflecting changes in the mucosal or submucosal layers, ostensibly not related to the motility control.

The Innate Immune System Modulates Intestinal VIP Expression

Because neuroimmune interactions play a key role in gut function[18,19] and MYD88-TRIF signaling is critical for TLR-mediated immune responses to bacteria,[20,21] we analyzed these gene expressions in germ-free and SPF mice. Jejunal *Tollip* and *Myd88* expression differed between germ-free and SPF mice (Figure 2*A*); therefore we assessed motility in *Myd88$^{-/-}$Trif$^{-/-}$* and wild-type (WT) mice. Although intestinal transit and jejunal EFS-induced contractility were similar between knockout and WT mice in the absence of microbiota, they differed between WT and *Myd88$^{-/-}$Trif$^{-/-}$* colonized mice (Figure 4*A* and *B*). VIP expression in jejunal myenteric plexus mirrored these results, with similar levels in germ-free conditions and higher levels in SPF WT mice (Figure 4*C*).

To validate these results, we assessed motility and contractility in germ-free *Myd88$^{-/-}$Trif$^{-/-}$* and WT mice before and after monocolonization with *E coli*. Although there were no differences between the 2 strains in germ-free condition, *E coli*-monocolonization increased intestinal transit and EFS-induced jejunal contractility in WT mice (Figure 4*E* and *F*), with no changes in *Myd88$^{-/-}$Trif$^{-/-}$* mice. In parallel, *E coli*-monocolonization increased VIP immunoreactivity in WT but not in *Myd88$^{-/-}$Trif$^{-/-}$* mice (Figure 4*G* and *H*), suggesting that the microbiota regulates small intestinal motility by modulating myenteric VIP expression through TLR-dependent pathways.

Microbial Modulation of Glial Cells Underlies Changes in VIP Expression

To investigate the role of innate immune cells in this process, we used fingolimod, a sphingosine-1-phosphate receptor modulator that inhibits activation and migration of immune cells including dendritic and enteric glial cells, and cosalane, which blocks activation of dendritic cells through CCR7.[22–24] Fingolimod, but not cosalane, decreased myenteric VIP levels in *E coli*-monocolonized mice (Figure 5*B*).

We then investigated presence of glial cells, identified by S100 calcium binding protein B (S100β) and glial fibrillary acidic protein immunoreactivity, and found they were co-localized with VIP nerves in SPF mice (Figure 5*A*). Similar to VIP expression, fingolimod, but not cosalane, attenuated the expression of myenteric S100β in *E coli*-monocolonized mice (Figure 5*C*). Furthermore, mirroring the results of intestinal transit and VIP expression, SPF and *E coli*-monocolonized mice had higher S100β levels than germ-free mice (Figure 5*D*).

To further explore the role of enteric glial cells in motility control, we used gliotoxin to inhibit their function. One-week intraperitoneal administration of gliotoxin in SPF mice resulted in a prolonged intestinal transit time accompanied by a decrease in VIP expression in the jejunal myenteric plexus (Figure 5*E* and *F*). All together, these data suggest that microbiota-glial cells interactions underlie changes in VIP expression and intestinal motility.

Presence of Microbiota Is Essential for Normal Intestinal Motility

To study whether the continuous presence of microbiota is required for regular intestinal VIP levels and gut motility, we used the transient bacterial colonizer *E coli HA107*[25] or treatment with nonabsorbable antibiotics. Ex–germ-free mice gavaged with *E coli HA107* (Figure 6*B*) displayed faster intestinal transit and higher VIP levels at day 14 after colonization, when bacteria were present in the gut. However, at day 42, after reverting to germ-free status, the intestinal transit and VIP expression decreased (Figure 6*B*). In contrast, mice monocolonized with *E coli JM83* (WT) displayed faster intestinal transit and higher VIP levels at both days 14 and 42 after colonization compared with germ-free mice (Figure 6*A*).
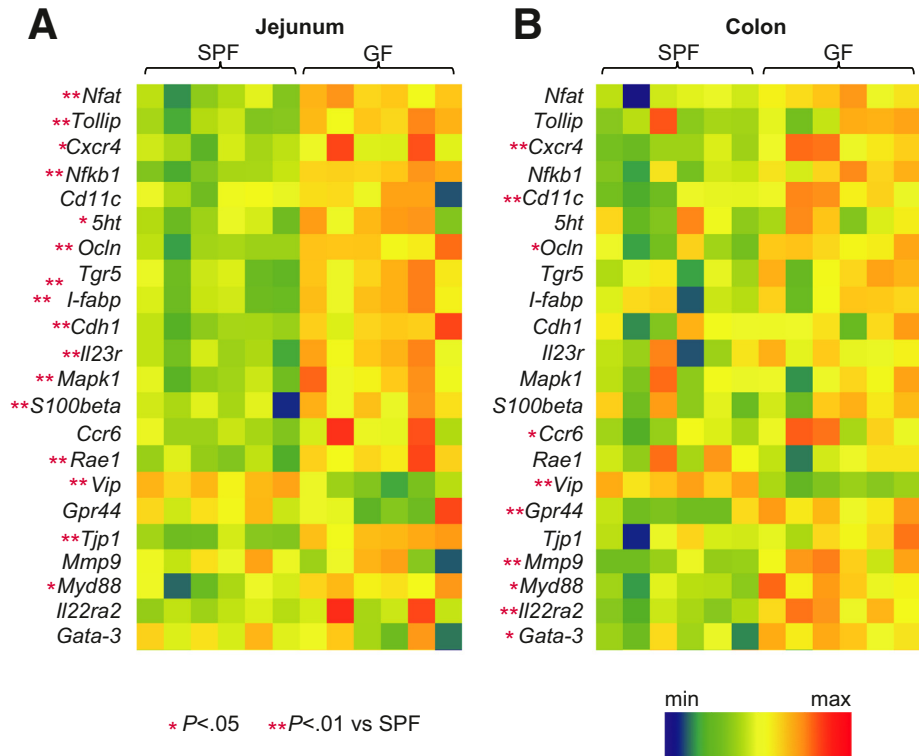
Figure 2. Neuroimmune genes affected by microbial colonization. (*A* and *B*) Heat map of neuroimmune genes, the expression of which differs in whole-thickness jejunum and colon tissues between SPF and GF mice (6 samples per group, each sample contains tissues from 2 mice). *Red* represents up-regulated genes, *blue* down-regulated genes. *$P < .05$, **$P < .01$.

Administration of broad-spectrum antibiotics to SPF mice (Figure 6*C*) resulted in slower intestinal transit and lower jejunal myenteric VIP immunoreactivity, both of which normalized 2 weeks later (Figure 6*C*). As shown previously,[26] antibiotics altered microbial profiles and reduced total bacterial counts (Figure 6*D* and *E*), which normalized 2 weeks later. This suggests that continuous presence of bacteria is required for normal motility, and that changes in the microbial load and profiles are dynamically reflected by changes in intestinal transit and myenteric VIP.

Small Intestinal VIP Is Decreased in Patients With Severe Constipation

To illustrate the clinical relevance of our findings, we examined VIP expression in full-thickness biopsy samples of small intestinal tissues from patients with established chronic intestinal pseudo-obstruction (CIPO), which is characterized by intractable constipation. Compared with small intestinal samples from control subjects, VIP expression was lower in CIPO specimens (Figure 6*F*), providing further support for its role in the regulation of gastrointestinal motility.

Discussion

Although the key role of microbiota in regulating gastrointestinal motility is well-established, the precise mechanisms are poorly understood. We show that gastric emptying is not affected by the microbiota, whereas intestinal transit differs between germ-free and colonized mice. The changes in transit are determined by the altered function of the small intestine, because most metallic beads were found in the jejunum and ileum. This was not due to the changes in myogenic function, because KCl-stimulated muscle contractility was similar between germ-free and colonized mice, but due to changes in its neural control. EFS-induced contraction and relaxation patterns were affected by the microbiota, with more pronounced relaxation and weaker contraction in germ-free mice, paralleled by acetylcholine release. Microbial influence differs between bacterial strains, because intestinal transit, acetylcholine release, and contractility were lower in *L rhamnosus*-monocolonized mice compared with those with *E coli* or complex SPF microbiota.

When investigating underlying mechanisms, there was no difference in ChAT expression between germ-free and SPF mice, suggesting that cholinergic nerves are not affected per se, but we found major differences in VIP gene expression. VIP acts on receptors located on smooth muscle to mediate relaxation,[27] but it also serves as a co-transmitter at cholinergic synapses in the small intestinal myenteric plexus,[17] activating jejunal cholinergic neurons.[28] Accordingly, VIP-deficient mice display decreased jejunal motility,[29] whereas VIP administration enhances motility as demonstrated previously[30] and in our study, supporting its role in excitatory pathways. We observed co-localization of jejunal myenteric VIP- and ChAT-immunoreactive neurons and found that pretreatment with VIP receptor antagonists increased relaxation and decreased contraction of jejunal tissues, demonstrating that VIP controls cholinergic nerves in the small intestine.

VIP is mainly expressed in the myenteric plexus, but it is also abundant in mucosal and submucosal layers.[28,31]

Colonic myenteric VIP immunoreactivity was not altered by the gut microbiota, but VIP gene expression was affected in whole-thickness colon tissues. This is in agreement with studies demonstrating that microbiota does not alter colonic myenteric VIP expression,[12] that colonic VIP receptors mainly localize at the mucosa,[32] and that VIP gene mutation
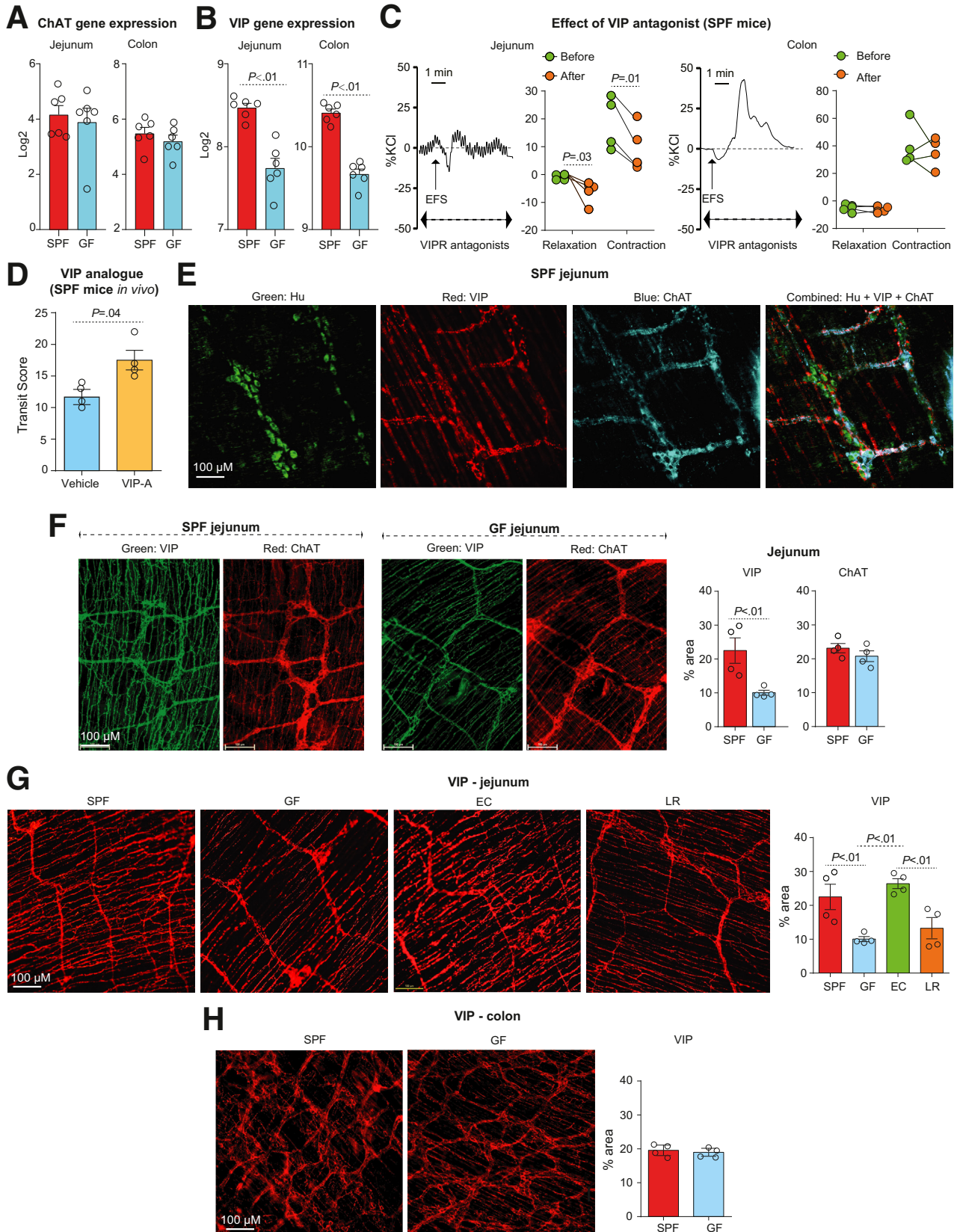
is associated with minimal changes in colon function.[29] Thus, although the effect of the microbiota on VIP expression in the colon is exerted in the mucosal layer, promoting colonic barrier homeostasis,[33] in the small intestine the VIP is linked to motility and cholinergic nerve control.

To further investigate the mechanisms underlying changes in intestinal motility, we colonized germ-free mice with a single Gram-negative (*E coli*) or Gram-positive (*Lactobacillus rhamnosus*) bacterial strain. Although more significant in *E coli*-colonized group, both increased small intestinal motility and VIP expression, confirming that both TLR4 and TLR2 pathways are involved in microbial control of gut motility and neural function.[8,9] MYD88/TRIF signaling pathways are downstream from both TLR 2 and 4 receptors, playing key roles in host innate immune responses to bacteria.[21,34,35] We found that *Myd88* gene expression differed between germ-free and SPF mice in WT mice, and that intestinal transit, jejunal contractility, and myenteric plexus VIP immunoreactivity were similar in germ-free and SPF *Myd88*^{-/-}*Trif*^{-/-} mice. Furthermore, *E coli*-monocolonization of germ-free *Myd88*^{-/-}*Trif*^{-/-} mice did not alter these parameters, demonstrating that TLR signaling mediates the microbial control of intestinal motility.

To identify innate immune cells involved in this process we used cosalane, which specifically inhibits dendritic cell activation,[24,36] and fingolimod, which inhibits activation and migration of immune cells including dendritic and enteric glial cells.[37–39] We found that fingolimod, but not cosalane, blocked increase in VIP expression after bacterial colonization, suggesting that enteric glial cells, rather than dendritic cells, are involved in this process. Enteric glial cells contribute to gut function maintenance, including motility, synaptic transmission, and neurogenesis, via dynamic interactions with immune cells and neurons.[40,41] Indeed, we found that glial cells shared the same localization and changes in density as VIP positive neurons, suggesting that they mediate the bacterial control of intestinal motility. Furthermore, specific inhibition of glial cell function with gliotoxin decreased VIP expression and prolonged intestinal transit time, further supporting the key role of glial cells. A denser immune cell network in the small intestine[42] and possibly different functional phenotypes of enteric glial cells in the small intestine compared with the colon[43] might be the reason why the microbial-immune crosstalk governs gastrointestinal motility mainly in the small intestine and not in the colon.

Immune responses can be long-lived in transiently colonized mice,[25] but it is unknown whether they are sufficient to maintain normal motility. We used *E coli HA107,* a triple auxotrophic mutant that colonizes the mouse intestine only transiently and is not detectable 48 hours after its last gavage,[25] to monocolonize germ-free mice. Although intestinal transit and VIP expression increased during colonization, both returned to values observed in germ-free mice 4 weeks later, suggesting that the immune priming associated with the microbial colonization is not sufficient, and that bacterial presence is needed to maintain normal intestinal motility.

The microbiota is involved in the maturation of enteric nervous system[11] and maintenance of its homeostasis.[44] In our experiments, administration of nonabsorbable antimicrobials to SPF mice decreased jejunal VIP levels and intestinal transit, which then normalized 2 weeks later, in parallel with microbiota profiles. This demonstrates that VIP expression in adult, conventionally raised mice is continuously and dynamically modulated by the gut microbiota.

To validate our findings clinically, we investigated levels of small intestinal VIP in a small set of patients with CIPO. CIPO is the "tip of the iceberg" of a wide spectrum of gastrointestinal motility disorders, and CIPO-affected patients suffer from intractable constipation.[45] We found that compared with control subjects, jejunal VIP levels are lower in patients with CIPO, thus extending our findings from mouse models into humans. These results are in agreement with multiple reports demonstrating that intestinal VIP is lower in patients with chronic constipation and higher in those with chronic diarrhea.[46,47] Interestingly, recent studies suggested that fecal microbiota transplantation improves symptoms in patients with intestinal dysmotility, including those with irritable bowel syndrome and CIPO,[48,49] and we hypothesize that these beneficial effects might be due, at least in part, to the microbial regulation of intestinal VIP.

In summary, we show that gut microbiota regulates gastrointestinal motility in a region-specific manner, with maximum effects seen in the small intestine. Specific bacterial strains exert differential effects, with major changes seen with *E coli* and minimum ones with *L rhamnosus*. Gut microbiota affects the function and structure of the jejunal enteric nervous system by modulating myenteric VIP, which in turn controls cholinergic nerves. This regulation is dependent on microbiota-innate immune system crosstalk, critically involving MYD88/TRIF-dependent pathways and enteric glia cells. Both the presence and stability of microbiota are essential to maintain myenteric VIP level and normal intestinal motility. Finally, we show that jejunal VIP levels are altered in patients with severe constipation, thus providing clinical relevance to our murine experiments.

Figure 3. (*See previous page*). **Effect of bacterial colonization on myenteric VIP and ChAT.** (*A and B*) *VIP* and *ChAT* gene expression assessed by Nanostring in tissues from SPF and GF mice (*each circle* represents a pooled sample from 2 mice). (*C*) Representative recordings and summary of EFS-induced responses of tissues from SPF mice (n = 4) before and after treatment with combined VIP receptor 1 and 2 antagonists. (*D*) In vivo intestinal transit scores of vehicle (n = 4) and VIP analogue (n = 4) treated SPF mice. (*E*) VIP- and ChAT-immunoreactive nerves immunolabeled with antibodies to HuC/D (*green*), VIP (*red*), and ChAT (*cyan*) at the jejunal myenteric plexus of a SPF mouse. (*F*) VIP- and ChAT-immunoreactive nerves visualized by double-immunolabeling with antibodies to VIP (*green*) and ChAT (*red*) in jejunal myenteric plexus of SPF (n = 4) and GF (n = 4) mice. (*G*) Representative photographs (*left*) and results (*right*) of VIP immunoreactivity in jejunal myenteric plexus of SPF (n = 4), GF (n = 4), EC (n = 4), and LR (n = 4) mice. (*H*) Representative photographs (*left*) and results (*right*) of VIP immunoreactivity in colon myenteric plexus of SPF (n = 4) and GF (n = 4) mice.
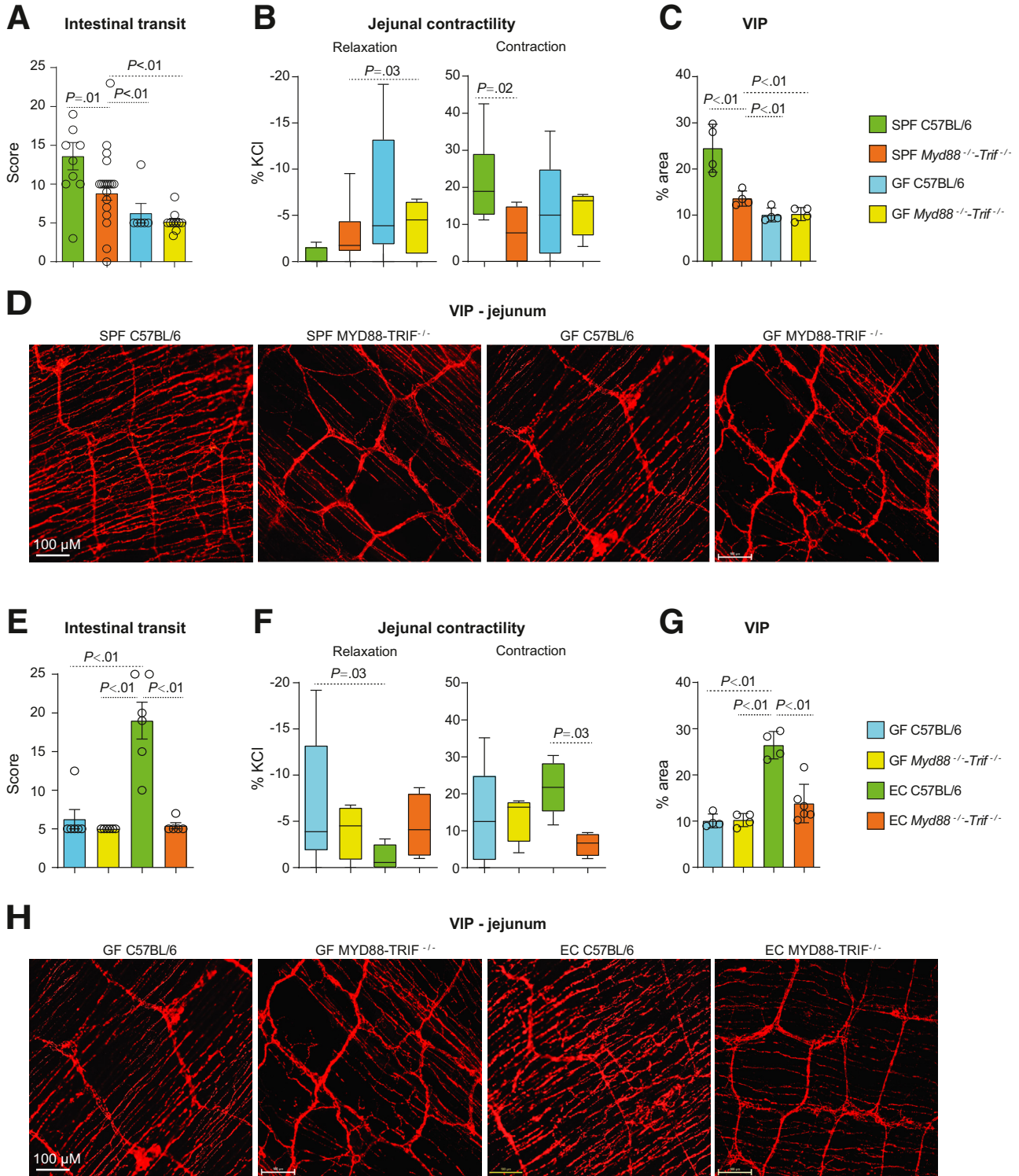
Figure 4. Role of MYD88/TRIF pathways in intestinal motility and jejunal myenteric VIP. (*A*) Intestinal transit scores of SPF C57BL/6 (n = 10), SPF *Myd88*^{-/-}*Trif*^{-/-} (n = 18), GF C57BL/6 (n = 6), and GF *Myd88*^{-/-}*Trif*^{-/-} (n = 10) mice. (*B*) EFS-induced responses of jejunum tissues from SPF C57BL/6 (n = 8), SPF *Myd88*^{-/-}*Trif*^{-/-} (n = 6), GF C57BL/6 (n = 11), and GF *Myd88*^{-/-}*Trif*^{-/-} (n = 4) mice. (*C*) VIP immunoreactivity in jejunum myenteric plexus of SPF C57BL/6 (n = 4), SPF *Myd88*^{-/-}*Trif*^{-/-} (n = 4), GF C57BL/6 (n = 4), and GF *Myd88*^{-/-}*Trif*^{-/-} (n = 4) mice. (*D*) Representative photographs of VIP immunoreactivity. (*E*) Intestinal transit scores of GF C57BL/6 and GF *Myd88*^{-/-}*Trif*^{-/-} mice before and after monocolonization with *E coli* (EC, n = 6 per group). (*F*) EFS-induced responses of jejunum tissues from GF C57BL/6 (n = 11), GF *Myd88*^{-/-}*Trif*^{-/-} (n = 6), EC C57BL/6 (n = 8), and EC *Myd88*^{-/-}*Trif*^{-/-} (n = 6) mice. (*G*) VIP immunoreactivity of GF C57BL/6 (n = 4), GF *Myd88*^{-/-}*Trif*^{-/-} (n = 4), EC C57BL/6 (n = 4), and EC *Myd88*^{-/-}*Trif*^{-/-} (n = 6) mice. (*H*) Representative photographs of VIP immunoreactivity.
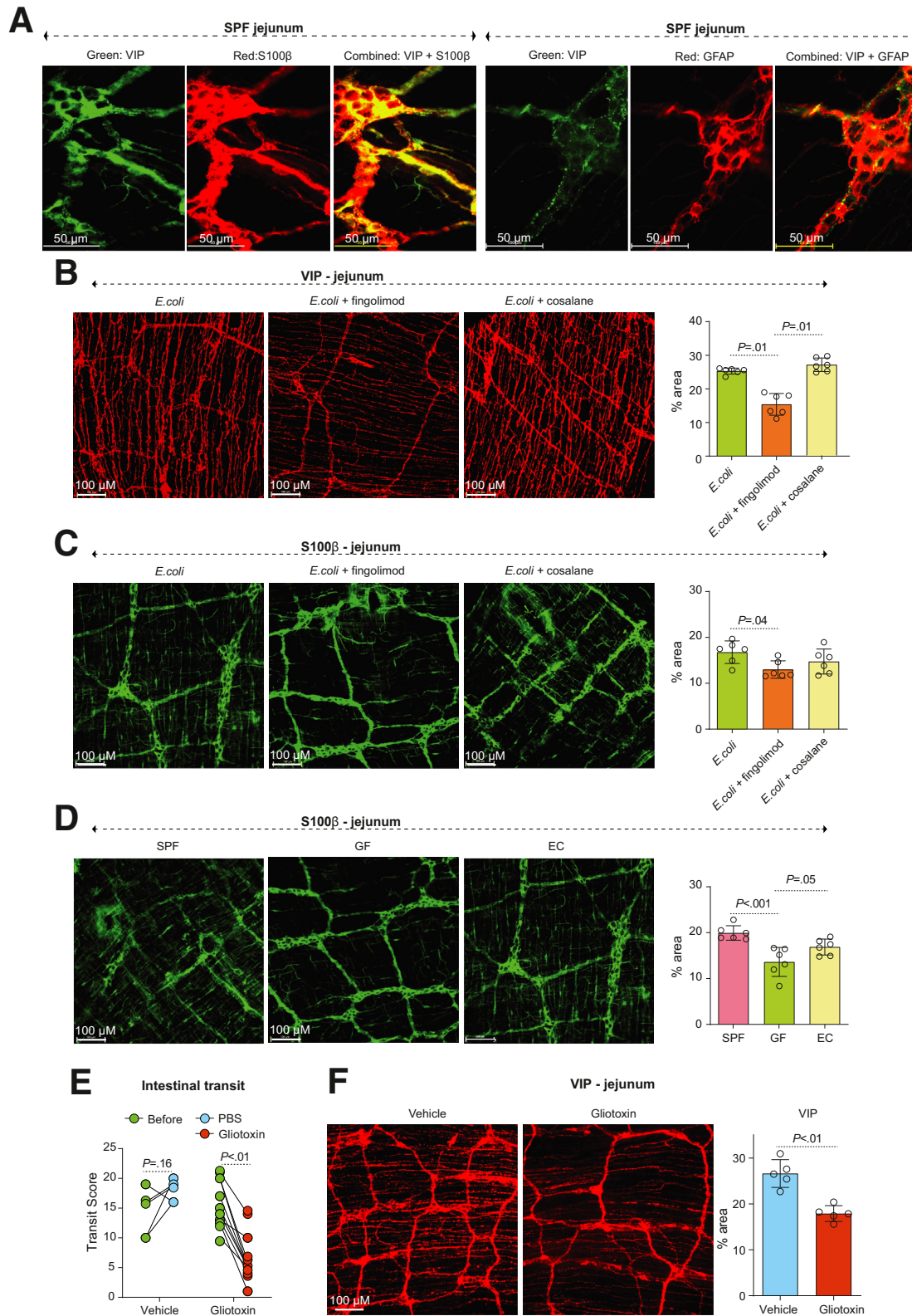
Figure 5. **Effect of immune blockade on jejunal myenteric plexus VIP and glial cells.** (*A*) VIP-immunoreactive nerves and glial cells visualized by double-immunolabeling with antibodies to VIP (*green*) and glial cells (*red*, S100β or glial fibrillary acidic protein [GFAP]) in jejunal myenteric plexus of SPF mouse. (*B*) Representative photographs and results of VIP immunoreactivity of *E coli*-monocolonized mice treated with saline (n = 6), fingolimod (n = 6), or cosalane (n = 6). (*C*) Representative photographs and results of S100β immunoreactivity (*green*) of *E coli*-monocolonized mice treated with saline (n = 6), fingolimod (n = 6), and cosalane (n = 6). (*D*) Representative photographs and results of S100β immunoreactivity of SPF (n = 6) and GF (n = 6) and *E coli*-monocolonized mice (n = 6). (*E*) In vivo transit scores of vehicle (n = 4) and gliotoxin (n = 10) treated SPF mice. (*F*) Representative photographs and results of VIP immunoreactivity of vehicles (n = 5) and gliotoxin applications (n = 5) to SPF mice.

Our data suggest that deeper understanding of microbiota-neuroimmune interactions in the small bowel could lead to better therapies to manage motility disorders. These could include identification and development of microbial therapeutics that modulate small intestinal VIP to treat chronic constipation and diarrhea.
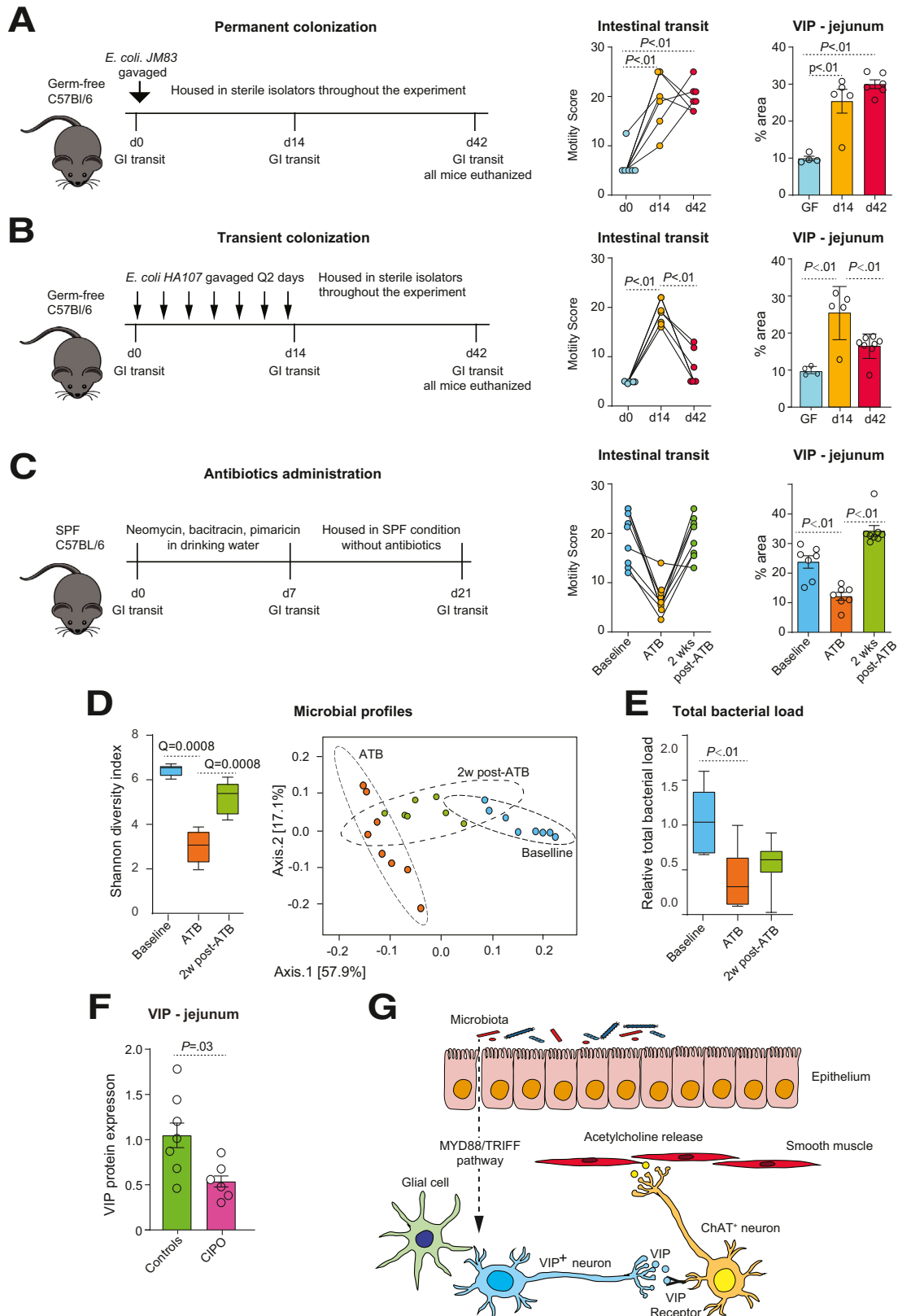
Methods

All animal experiments were approved by the McMaster University Animal Care Committee (AUP 18-08-35). The clinical study was approved by the Ethics Committee of St. Orsola-Malpighi Hospital of Bologna, Italy (Protocol No. 50/2012/O/Sper (EM/146/2014/O)). All patients and healthy controls provided written informed consent to participate.

Gnotobiotic Mice

$MyD88^{-/-}$; $Ticam1^{-/-}$ mice on a C57BL/6 background were provided by B. A. Beutler (La Jolla, CA). SPF C57BL/6 mice were purchased from Taconic. Germ-free C57BL/6 and $MyD88^{-/-}$; $Ticam1^{-/-}$ mice were rederived at the Farncombe Family University Axenic Gnotobiotic Unit (AGU) of the Central Animal Facility, McMaster University, and maintained axenic in sterile isolators. To ensure sterility, handling of germ-free mice was carried out under axenic conditions as described previously.[50] All mice were maintained on a 12-hour day/night cycle with free access to food and water. Germ-free and monocolonization status was assessed regularly by direct bacteriology, immunofluorescence, and 16S polymerase chain reaction testing for culturable and unculturable organisms.

Bacterial Colonization of Germ-Free Mice

Germ-free mice (both sexes) were monocolonized with 10^9 colony-forming units of *E coli JM83*, *Lactobacillus rhamnosus X-32.2*, or *E coli HA107* via intragastric gavage (200 μL/mouse). *E coli HA107* strain is a mutant form of the parental strain *E coli JM83*, which is not able to synthesize meso-diaminopimelic acid (m-DAP; Sigma-Aldrich) or D-isomer of alanine (D-Ala; Sigma-Aldrich) required in the peptidoglycan crosslink of the cell wall and thus only transiently colonizes (12–48 hours) mouse intestine.[25] The transient colonizer *E coli HA107* was gavaged 3 times weekly for 2 weeks (Figure 6B). The permanent colonizer *E coli JM83* (Figure 6A) and *Lactobacillus rhamnosus X-32.2* were gavaged once. All monocolonized mice were maintained in sterile isolators within the Axenic Gnotobiotic Unit.

E coli JM83 was grown in Luria Bertani (LB) broth (Sigma-Aldrich), and *E coli HA107* was grown in LB broth supplemented with D-Ala (200 μg/mL)/m-DAP (50 μg/mL) and incubated with shaking at 160 rpm at 37°C for 12 hours. *Lactobacillus rhamnosus X-32.2* was grown in deMan, Rogosa, and Sharpe (MRS) broth, anaerobically, at 37°C for 18 hours. Bacteria were harvested by centrifugation (15 minutes, 3500g) in a 400-mL sterile flask, washed in sterile phosphate-buffered saline (PBS), and concentrated, all under a sterile laminar flow hood. The bacterial suspensions were sealed in sterile tubes, with the outside surface kept sterile, and imported into sterile isolators.

To assess colonization or de novo germ-free status after transient colonization, cecal contents were plated on LB agar plates (with or without supplementation with m-DAP and D-Ala) or on MRS agar plates and incubated for 48 hours.

To confirm the colonization efficiency of *E coli JM83* and *L rhamnosus*, the ceca from 5 mice per group were thawed, and the contents were diluted 10 times (w/v) with sterile PBS and then serially diluted again (10-fold) with PBS until 10^{-9}. Diluted samples (100 μL; diluted to 10^{-9}, 10^{-7}, and 10^{-5}) were then plated onto MRS (for *L rhamnosus*) or brain-heart infusion (for *E coli JM83*) plates and incubated aerobically or anaerobically for 48 hours. After 48 hours the colonies that grew on the plates were counted, and colony-forming units/mL were calculated. We saw no differences in the colonization levels between the 2 bacterial strains ($4.82 \times 10^9 \pm 3.71 \times 10^9$ for *E coli JM83*; $3.44 \times 10^{10} \pm 4.58 \times 10^{10}$ for *L rhamnosus*).

Gnotobiotic Husbandry

Isolators that housed germ-free mice underwent strict protocols to prevent contamination of microbes from animal handlers or environment. Samples of the imported materials were taken for aerobic and anaerobic bacterial culture regularly. Feces and bedding were taken from the isolator for direct bacteriology, microscopy, and 16S polymerase chain reaction testing of intestinal contents to test for culturable and unculturable organisms. Cecal contents from monocolonized mice were suspended and serially diluted in sterile 1× PBS and plated on LB or MRS agar plates for 48 hours. Cecal contents from mice treated with *E coli HA107* strain were incubated on LB plates supplemented with m-DAP and D-Ala. To confirm de novo germ-free status after colonizing with *E coli HA107*, cecal contents were plated on supplemented LB agar plate 2 and 4 weeks after the last gavage.

Figure 6. (*See previous page*). **Gut microbiota is essential for normal intestinal transit and jejunal myenteric VIP levels.** (*A*) Experimental design for permanent colonization of GF mice with *E coli* JM83 (*left*); intestinal transit scores for GF mice before (d0) and after colonization with *E coli* JM83 at day 14 (d14) and day 42 (d42, n = 6); VIP expression of GF mice before (d0, n = 4) and after colonization with *E coli* JM83 at day 14 (d14, n = 5) and at day 42 (d42, n = 6). (*B*) Experimental design for transient colonization of GF mice with *E coli* HA107 (*left*); intestinal transit scores of GF mice (n = 11) before and after 2-week monocolonization (d14) with the transient colonizer *E coli* HA107 and 4 weeks later, when mice reverted to GF status (d42, n = 7); VIP expression of GF mice (n = 4), mice monocolonized with *E coli* HA107 (d14, n = 5), and after reverting to GF status (d42, n = 8). (*C*) Experimental design for antibiotic treatment of SPF mice (*left*); intestinal transit scores of SPF mice before (baseline) and after 1 week of antibiotics (ATB) and after 2-week washout (2-week post-ATB, n = 8); VIP expression in SPF mice before (n = 7) and after antibiotics (n = 7) and after 2-week washout (n = 8). (*D*) Microbiota profiles in antibiotic treated mice. Shannon diversity index and weighted unifrac PCoA plot at baseline, after 1 week of ATB, and after 2-week washout. (*E*) Total bacterial load at baseline, after 1 week of ATB, and after 2-week washout period. (*F*) VIP protein expression in full-thickness biopsy jejunum tissues from controls (n = 7) and CIPO patients (n = 6). (*G*) Schematic overview of gut microbiota-neuroimmune interactions governing intestinal transit.

Antibiotics Administration

Neomycin (Sigma-Aldrich) and bacitracin (Sigma-Aldrich) were dissolved in distilled water (both at 5 mg/mL), pimaricin (Sigma-Aldrich) was added (5 μL/mL), and the solution was filtered sterile. Antibiotics were administered for 1 week and changed every 48 hours.

Gastric Emptying

Gastroduodenal motility was assessed using video image analysis as described previously.[51] Briefly, mice were gavaged with 0.2 mL of 40% barium solution, placed in custom Plexiglas restrainers, and videofluoroscoped for 4 minutes. Video images were analyzed using ImageJ. Gastric emptying was assessed in single images by manually outlining the border of stomach and measuring gastric area and its mean optical density. The amount of barium at 0 and 4 minutes was assessed by multiplying the gastric area by the mean optical density in each image. Gastric emptying was expressed as a percentage of barium expelled from the stomach in 4 minutes.

Gastrointestinal Transit

Gastrointestinal transit was assessed using video-fluoroscopy as described previously.[52] Briefly, 5 steel beads (0.79-mm diameter; Bal-tec) with 40% barium solution (0.1 mL) were gavaged into each mouse. A second barium gavage (0.2 mL) was performed 170 minutes later. Ten minutes later, the mouse was placed in a custom-built Plexiglas restrainer and videofluoroscoped. Video images were analyzed using ImageJ. Each bead was assigned a score depending on its location within the gastrointestinal tract, and their scores were added together to calculate a total transit score.

Gene Expression

RNA was extracted by RNeasy Mini Kit (Qiagen, Toronto, Canada); DNase digestion was performed by RNase-free DNase (Qiagen). A custom Nanostring codeset run according to manufacturer's instructions was analyzed by nSolver 4.0 (NanoString Technologies, Seattle, WA) and by Ingenuity Pathway software (Qiagen).

Muscle Contractility

Muscle contractility was assessed as previously described[53] after stimulation with KCl, carbachol, EFS, and VIP receptor antagonist 1 (Acetyl-(D-Phe^2,Lys^{15}, Arg^{16},Leu^{27})-VIP-(1-7)-GRF(8-27)trifluoroacetate, 10 μmol/L) and 2 (VPAC2):Myristoyl-(Lys$^{12.27.28}$)-VIP-Gly-Gly-Thr-tri-fluoroacetate, 10 μmol/L; Bachem, Torrance, CA), using multichannel transducer system (MLT0201, Panlab s.l, Spain).

Muscle contractility was measured as previously described.[53] Briefly, tissues of the jejunum and mid colon were kept in oxygenated (95% O_2, 5% CO_2) Krebs solution containing (in mmol/L) 120.9 NaCl, 1.2 NaH$_2$PO$_4$, 15.5 NaHCO$_3$, 5.9 KCl, 2.5 CaCl$_2$, 1.2 MgCl$_2$, and 11.1 glucose at pH 7.4. One-centimeter sections of the gut were removed from the jejunum, beginning at the ligament of Treitz and

proceeding distally, and mid colon. The lumen of each segment was flushed gently with Krebs buffer before the insertion of short Silastic tubing (0.065 inches OD, 0.030 inches ID; Dow Corning, Midland, MI) into each end. The tubing was then tied in position with surgical silk. Segments were hung in the longitudinal axis and attached to a force transducer (MLT0201, 5 mg–25 g, Panlab s.l, Spain). Tissues were equilibrated for 30 minutes in oxygenated Krebs solution and then stretched with 1 mg force before the experiment was started. Muscle strips were then stimulated with 50 mmol/L KCl, carbachol, VIP receptor antagonists, and EFS (30 V, 5 Hz, 0.5 mS), and responses were recorded. VIP receptor antagonists of type 1 (VPAC1), Acetyl-(D-Phe^2, Lys^{15}, Arg^{16}, Leu^{27})-VIP(1-7)-GRF(8-27) trifluoroacetate salt and antagonists of type 2 (VPAC2): Myristoyl-(Lys$^{12.27.28}$)-VIP-Gly-Gly-Thr(free acid) trifluoroacetate salt were purchased from Bachem Inc. The force was expressed in percent, assigning the levels obtained at rest and at peak of KCl-induced contraction as 0% and 100%, respectively.

[^{3}H]-Choline Release Measurement

Small intestine and colon were removed and cut in half. Longitudinal muscle–myenteric plexus preparations were dissected, placed in oxygenated Krebs solution, and pre-incubated with 0.5 μmol/L of [^{3}H]-choline for 40 minutes at 37°C as previously described.[16,52] Tissues were then transferred to the superfusion chambers and perfused with Krebs solution with 5 mmol/L hemicholinium-3 at a rate of 1 mL^{-1} min. Aliquots were collected every 2 minutes for 80 minutes using Spectrum Spectra/Chrom CF-1 Fraction Collector (FL). [3H]-Acetylcholine release was induced by EFS (30 V, 10 Hz, 0.5 mS) for 1 minute (S48 stimulator; Grass, Quincy, MA) or by adding 50 mmol/L KCl to the superfusate for 6 minutes and then measured using a Beckman scintillation counter (LS5801; Beckman Instruments, Fullerton, CA) at a counting efficiency of 35% and expressed as a fraction of the total [3H] in the tissue. Acetylcholine release was expressed in %, assigning the levels of choline release at baseline and at peak level induced by KCl as 0% and 100%, respectively.

VIP Analogue In Vivo Application

VIP analogue,[54] [Ala2,8,9,11,19,22,24,25,27,28]-VIP (BioCrick BioTech, Chengdu, China), 5 μg/day or vehicle (PBS) was administered by continuous subcutaneous infusion at 1 μL/h for 3 days via osmotic pumps (Alzet Model 2001; Durect Corporation, Palo Alto, CA). The osmotic pump was incubated in PBS for 24 hours at 37°C before implantation and was implanted dorsally using isoflurane anesthesia. Transit time was measured on day 3.

Gliotoxin In Vivo Application

Gliotoxin fluorocitrate solution was prepared as described before.[55] D,L-fluorocitric acid, Ba, salt (Sigma-Aldrich) 8 mg was dissolved in 1 mL of 0.1 mmol/L HCL. Two to three drops of 0.1 mmol/L Na$_2$SO$_4$ were added to precipitate the Ba^{2+}. Two milliliters of 0.1 mmol/L Na$_2$HPO$_4$ was added, and the suspension was centrifuged at 1000g for

5 minutes. The supernatant was diluted with PBS to the final concentration, and the pH was adjusted to 7.4. The gliotoxin fluorocitrate solution (20 μmol/kg/day) or PBS was injected intraperitoneally daily for 7 days. Gastrointestinal transit time was measured on days 0 (before first injection) and 7.

Immunohistochemistry Assessment

Whole mounts of intestine were collected immediately after death, cut open longitudinally, and pinned serosal side down on Petri dishes. The tissues were fixed for 2 hours at room temperature in 4% phosphate-buffered formaldehyde (pH 7.4) and then washed in PBS. Laminar preparations of longitudinal muscle with adherent myenteric plexus were obtained by dissections. Tissues were then permeabilized and blocked by incubation in PBS containing 0.4% Triton X-100 and 5% normal bovine serum. Primary antibodies including rabbit polyclonal immunoglobulin G antibodies to VIP (dilution 1:5000; Immunostar), biotinylated mouse monoclonal antibodies to human neuronal protein HuC/HuD (dilution 1:100; Molecular Probes, Invitrogen), goat polyclonal ChAT antibodies (dilution 1:100; Invitrogen), and S100 beta antibody (dilution 1:500, GeneTex) were applied overnight at 4°C. Antibody binding was detected with donkey anti-rabbit antibodies labeled with Alexa 555 (1:1000; Molecular Probes), streptavidin labeled with Alexa 488 (1:200; Molecular Probes), donkey anti-goat antibodies labeled with Alexa 555 (1:200; Molecular Probes), or with donkey anti-goat antibodies labeled with Alexa 647 (1:100; Molecular Probes) by incubation for 2 hours at room temperature. No immunostaining was observed when primary antibodies were omitted. Tissue sections were mounted with Vectashield medium (Vector Laboratories Canada Inc, Burlington, ON, Canada). Raw pictures in gray scale were loaded into FIJI ImageJ, and signals were normalized by setting threshold as 0-1. Staining level was expressed in percentage by the ratio of VIP-positive area in a 1 cm^2 image.

Microbiota Analysis

Total genomic DNA was extracted from cecal samples, and the V3 region of the 16S rRNA gene amplified and Illumina sequencing was performed as previously described.[56,57] The data were analyzed following the pipelines of dada2,[58] QIIME2,[59] and Phyloseq package (1.30) for R (3.6.3).[60] Taxonomic assignments were performed using the RDP classifier with the Greengenes (2013) training set.[61,62] Analyses were done using QIIME2, Phyloseq package (1.30), and SPSS software v.23. All results were corrected for multiple comparisons, allowing 5% false discovery rate.

Total bacterial load was measured by quantitative polymerase chain reaction with the primers 926F 5′-AAACT-CAAAKGAATTGACGG-3′ and 1062R 5′-CTCACRRCACGAGCTGAC-3′ for the V6 region of the 16S rRNA. The data were expressed as total bacterial load relative to the average of the control population (baseline water): E (Ct test- Ct calibrator), where E was the efficiency of each PCR (1.97-2), and the calibrator was the average of the Ct of all baseline controls.

Patient Samples

Full-thickness jejunal samples were collected from well-characterized CIPO patients with degenerative neuropathy (total n = 6, female = 3; age range: 30–73 years) investigated at St. Orsola-Malpighi Hospital, Bologna, Italy. Control samples were obtained from patients undergoing resection due to non-complicated intestinal tumors (total n = 8, female = 3; age range: 48–68 years).

Proteins were extracted, separated, and transferred onto nitrocellulose membrane (Thermo Fisher Scientific). Rabbit polyclonal anti-VIP antibody (Abcam, Cambridge, UK) was used as primary and anti-rabbit horseradish peroxidase–conjugated antibody (Sigma-Aldrich) as secondary. Visualization was performed by ECL Western Blotting Substrate (Thermo Fisher Scientific) on iBrigh FL1500 Imaging System (Invitrogen).

Human VIP Protein Assessment

Proteins were extracted from 0.5 g of each jejunal sample using TPER tissue protein extraction reagent with protease inhibitor cocktail (Thermo Fisher Scientific). Total protein was quantified using a Nano Drop 2000 spectrophotometer (Thermo Fisher Scientific). Proteins were separated using 12% acrylamide sodium dodecyl sulfate–polyacrylamide gel electrophoresis in reducing conditions and transferred onto nitrocellulose membrane (Thermo Fisher Scientific) overnight at 12 mV. Membranes were blocked with a buffer containing 5% fat-free milk and then incubated overnight at 4°C with rabbit polyclonal anti-VIP antibody (ab227850; Abcam). Anti-rabbit horseradish peroxidase–conjugated secondary antibody (Sigma-Aldrich) was applied for 2 hours at room temperature. Immunoreactive bands were visualized by ECL Western Blotting Substrate (Thermo Fisher Scientific) on iBrigh FL1500 Imaging System (Invitrogen). The iBright software was also used to quantify the total protein signal in each lane, stained with Ponceau S, used as reference.

Statistical Analysis

Data analyses were performed using GraphPad Prism 6.0, nSolver 4.0, and Microsoft Excel 2016. Data are presented as medians (interquartile range) or means ± standard deviation; statistical testing was performed using parametric or non-parametric tests as appropriate.

References

1. Ma C, Congly SE, Novak KL, et al. Epidemiologic burden and treatment of chronic symptomatic functional bowel disorders in the United States: a nationwide analysis. Gastroenterology 2021;160:88–98 e4.

2. Margolis KG, Cryan JF, Mayer EA. The microbiota-gut-brain axis: from motility to mood. Gastroenterology 2021;160:1486–1501.

3. O'Mahony SM, Felice VD, Nally K, et al. Disturbance of the gut microbiota in early-life selectively affects visceral pain in adulthood without impacting cognitive or anxiety-related behaviors in male rats. Neuroscience 2014; 277:885–901.

4. Geuking MB, Cahenzli J, Lawson MA, et al. Intestinal bacterial colonization induces mutualistic regulatory T cell responses. Immunity 2011;34:794–806.

5. Johansson MEV, Gustafsson JK, Holmen-Larsson J, et al. Bacteria penetrate the normally impenetrable inner colon mucus layer in both murine colitis models and patients with ulcerative colitis. Gut 2014;63:281–291.

6. Husebye E, Hellstrom PM, Sundler F, et al. Influence of microbial species on small intestinal myoelectric activity and transit in germ-free rats. Am J Physiol Gastrointest Liver Physiol 2001;280:G368–G380.

7. Berseth CL. Gastrointestinal motility in the neonate. Clin Perinatol 1996;23:179–190.

8. Anitha M, Vijay-Kumar M, Sitaraman SV, et al. Gut microbial products regulate murine gastrointestinal motility via Toll-like receptor 4 signaling. Gastroenterology 2012; 143:1006–1016 e4.

9. Yarandi SS, Kulkarni S, Saha M, et al. Intestinal bacteria maintain adult enteric nervous system and nitrergic neurons via toll-like receptor 2-induced neurogenesis in mice. Gastroenterology 2020;159:200–213.e8.

10. Caputi V, Marsilio I, Cerantola S, et al. Toll-like receptor 4 modulates small intestine neuromuscular function through nitrergic and purinergic pathways. Front Pharmacol 2017;8:350.

11. De Vadder F, Grasset E, Manneras Holm L, et al. Gut microbiota regulates maturation of the adult enteric nervous system via enteric serotonin networks. Proc Natl Acad Sci U S A 2018;115:6458–6463.

12. Obata Y, Castano A, Boeing S, et al. Neuronal programming by microbiota regulates intestinal physiology. Nature 2020;578:284–289.

13. Agace WW, McCoy KD. Regionalized development and maintenance of the intestinal adaptive immune landscape. Immunity 2017;46:532–548.

14. Muller PA, Matheis F, Schneeberger M, et al. Microbiota-modulated CART(+) enteric neurons autonomously regulate blood glucose. Science 2020;370:314–321.

15. Bercik P, De Giorgio R, Blennerhassett P, et al. Immune-mediated neural dysfunction in a murine model of chronic Helicobacter pylori infection. Gastroenterology 2002;123:1205–1215.

16. De Palma G, Blennerhassett P, Lu J, et al. Microbiota and host determinants of behavioural phenotype in maternally separated mice. Nature Communications 2015;6:7735.

17. Willard AL. A vasoactive intestinal peptide-like cotransmitter at cholinergic synapses between rat myenteric neurons in cell culture. J Neurosci 1990;10:1025–1034.

18. Matheis F, Muller PA, Graves CL, et al. Adrenergic signaling in muscularis macrophages limits infection-induced neuronal loss. Cell 2020;180:64–78 e16.

19. Barajon I, Serrao G, Arnaboldi F, et al. Toll-like receptors 3, 4, and 7 are expressed in the enteric nervous system and dorsal root ganglia. J Histochem Cytochem 2009; 57:1013–1023.

20. Karmarkar D, Rock KL. Microbiota signalling through MyD88 is necessary for a systemic neutrophilic inflammatory response. Immunology 2013;140:483–492.

21. Fitzgerald KA, Palsson-McDermott EM, Bowie AG, et al. Mal (MyD88-adapter-like) is required for Toll-like receptor-4 signal transduction. Nature 2001;413: 78–83.

22. Choi JW, Gardell SE, Herr DR, et al. FTY720 (fingolimod) efficacy in an animal model of multiple sclerosis requires astrocyte sphingosine 1-phosphate receptor 1 (S1P1) modulation. Proc Natl Acad Sci U S A 2011; 108:751–756.

23. Luessi F, Kraus S, Trinschek B, et al. FTY720 (fingolimod) treatment tips the balance towards less immunogenic antigen-presenting cells in patients with multiple sclerosis. Mult Scler 2015;21:1811–1822.

24. Hull-Ryde EA, Porter MA, Fowler KA, et al. Identification of cosalane as an inhibitor of human and murine CC-chemokine receptor 7 signaling via a high-throughput screen. SLAS Discov 2018;23:1083–1091.

25. Hapfelmeier S, Lawson MA, Slack E, et al. Reversible microbial colonization of germ-free mice reveals the dynamics of IgA immune responses. Science 2010; 328:1705–1709.

26. Bercik P, Denou E, Collins J, et al. The intestinal microbiota affect central levels of brain-derived neurotropic factor and behavior in mice. Gastroenterology 2011; 141:599–609, e1–e3.

27. Crist JR, He XD, Goyal RK. Both ATP and the peptide VIP are inhibitory neurotransmitters in guinea-pig ileum circular muscle. J Physiol 1992;447:119–131.

28. Fung C, Unterweger P, Parry LJ, et al. VPAC1 receptors regulate intestinal secretion and muscle contractility by activating cholinergic neurons in guinea pig jejunum. Am J Physiol Gastrointest Liver Physiol 2014; 306:G748–G758.

29. Lelievre V, Favrais G, Abad C, et al. Gastrointestinal dysfunction in mice with a targeted mutation in the gene encoding vasoactive intestinal polypeptide: a model for the study of intestinal ileus and Hirschsprung's disease. Peptides 2007;28:1688–1699.

30. Shi XZ, Sarna SK. Gene therapy of Cav1.2 channel with VIP and VIP receptor agonists and antagonists: a novel approach to designing promotility and antimotility agents. Am J Physiol Gastrointest Liver Physiol 2008; 295:G187–G196.

31. Krueger D, Michel K, Zeller F, et al. Neural influences on human intestinal epithelium in vitro. J Physiol 2016; 594:357–372.

32. Jayawardena D, Guzman G, Gill RK, et al. Expression and localization of VPAC1, the major receptor of vasoactive intestinal peptide along the length of the intestine. Am J Physiol Gastrointest Liver Physiol 2017; 313:G16–G25.

33. Wu X, Conlin VS, Morampudi V, et al. Vasoactive intestinal polypeptide promotes intestinal barrier homeostasis and protection against colitis in mice. PLoS One 2015; 10:e0125225.

34. Ignacio A, Morales CI, Camara NO, et al. Innate sensing of the gut microbiota: modulation of inflammatory and autoimmune diseases. Frontiers in Immunology 2016; 7:54.

35. Yamamoto M, Sato S, Hemmi H, et al. Role of adaptor TRIF in the MyD88-independent toll-like receptor signaling pathway. Science 2003;301:640–643.

36. Fowler KA, Li K, Whitehurst CB, et al. The ex vivo treatment of donor T cells with cosalane, an HIV therapeutic and small-molecule antagonist of CC-chemokine receptor 7, separates acute graft-versus-host disease from graft-versus-leukemia responses in murine hematopoietic stem cell transplantation models. Biol Blood Marrow Transplant 2019;25:1062–1074.

37. Lee CW, Choi JW, Chun J. Neurological S1P signaling as an emerging mechanism of action of oral FTY720 (fingolimod) in multiple sclerosis. Arch Pharm Res 2010;33:1567–1574.

38. Chun J, Hartung HP. Mechanism of action of oral fingolimod (FTY720) in multiple sclerosis. Clin Neuropharmacol 2010;33:91–101.

39. Zeng X, Wang T, Zhu C, et al. Topographical and biological evidence revealed FTY720-mediated anergy-polarization of mouse bone marrow-derived dendritic cells in vitro. PLoS One 2012;7:e34830.

40. Gulbransen BD, Sharkey KA. Novel functional roles for enteric glia in the gastrointestinal tract. Nature Reviews Gastroenterology Hepatology 2012;9:625–632.

41. Sharkey KA. Emerging roles for enteric glia in gastrointestinal disorders. J Clin Invest 2015;125:918–925.

42. Mowat AM, Agace WW. Regional specialization within the intestinal immune system. Nature Reviews Immunology 2014;14:667–685.

43. Seguella L, Gulbransen BD. Enteric glial biology, intercellular signalling and roles in gastrointestinal disease. Nature Reviews Gastroenterology Hepatology 2021;18:571–587.

44. Hung LY, Boonma P, Unterweger P, et al. Neonatal antibiotics disrupt motility and enteric neural circuits in mouse colon. Cell Mol Gastroenterol Hepatol 2019;8:298–300 e6.

45. Di Nardo G, Di Lorenzo C, Lauro A, et al. Chronic intestinal pseudo-obstruction in children and adults: diagnosis and therapeutic options. Neurogastroenterol Motil 2017;29.

46. Koch TR, Carney JA, Go L, et al. Idiopathic chronic constipation is associated with decreased colonic vasoactive intestinal peptide. Gastroenterology 1988;94:300–310.

47. Sohn W, Lee OY, Lee SP, et al. Mast cell number, substance P and vasoactive intestinal peptide in irritable bowel syndrome with diarrhea. Scand J Gastroenterol 2014;49:43–51.

48. Gu L, Ding C, Tian H, et al. Serial frozen fecal microbiota transplantation in the treatment of chronic intestinal pseudo-obstruction: a preliminary study. J Neurogastroenterol Motil 2017;23:289–297.

49. El-Salhy M, Hatlebakk JG, Gilja OH, et al. Efficacy of faecal microbiota transplantation for patients with irritable bowel syndrome in a randomised, double-blind, placebo-controlled study. Gut 2020;69:859–867.

50. De PG, Blennerhassett P, Lu J, et al. Microbiota and host determinants of behavioural phenotype in maternally separated mice. Nat Commun 2015;6:7735.

51. Bercik P, Wang L, Verdu EF, et al. Visceral hyperalgesia and intestinal dysmotility in a mouse model of post-infective gut dysfunction. Gastroenterology 2004;127:179–187.

52. Jacobson K, McHugh K, Collins SM. The mechanism of altered neural function in a rat model of acute colitis. Gastroenterology 1997;112:156–162.

53. Vallance BA, Blennerhassett PA, Collins SM. Increased intestinal muscle contractility and worm expulsion in nematode-infected mice. Am J Physiol 1997;272(Pt 1):G321–G327.

54. Igarashi H, Ito T, Mantey SA, et al. Development of simplified vasoactive intestinal peptide analogs with receptor selectivity and stability for human vasoactive intestinal peptide/pituitary adenylate cyclase-activating polypeptide receptors. J Pharmacol Exp Ther 2005;315:370–381.

55. Hayakawa K, Nakano T, Irie K, et al. Inhibition of reactive astrocytes with fluorocitrate retards neurovascular remodeling and recovery after focal cerebral ischemia in mice. J Cereb Blood Flow Metab 2010;30:871–882.

56. Bartram AK, Lynch MD, Stearns JC, et al. Generation of multimillion-sequence 16S rRNA gene libraries from complex microbial communities by assembling paired-end illumina reads. Appl Environ Microbiol 2011;77:3846–3852.

57. Whelan FJ, Surette MG. A comprehensive evaluation of the sl1p pipeline for 16S rRNA gene sequencing analysis. Microbiome 2017;5:100.

58. Callahan BJ, McMurdie PJ, Rosen MJ, et al. DADA2: high-resolution sample inference from Illumina amplicon data. Nat Methods 2016;13:581–583.

59. Bolyen E, Rideout JR, Dillon MR, et al. Reproducible, interactive, scalable and extensible microbiome data science using QIIME 2. Nat Biotechnol 2019;37:852–857.

60. McMurdie PJ, Holmes S. Phyloseq: an R package for reproducible interactive analysis and graphics of microbiome census data. PLoS One 2013;8:e61217.

61. Wang Q, Garrity GM, Tiedje JM, et al. Naive Bayesian classifier for rapid assignment of rRNA sequences into the new bacterial taxonomy. Appl Environ Microbiol 2007;73:5261–5267.

62. DeSantis TZ, Hugenholtz P, Larsen N, et al. Greengenes, a chimera-checked 16S rRNA gene database and workbench compatible with ARB. Appl Environ Microbiol 2006;72:5069–5072.

Correspondence
Address correspondence to: Premysl Bercik, MD, Farncombe Family Digestive Health Research Institute, Department of Medicine, McMaster University, HSC 3N9, Hamilton, Ontario, Canada. e-mail: bercikp@mcmaster.ca.